Breakdown of Dynamic Scaling of Disclination Loop Decay Biased by Electrohydrodynamic Convection in a Nematic Liquid Crystal

H. M. Shehadeh and J. P. McClymer

Department of Physics and Astronomy, University of Maine, Orono, Maine 04469-5709

(Received 23 August 1996)

Electrohydrodynamic convection in the nematic liquid crystal MBBA in the presence of a competing magnetic field produces disclination loops in the two dynamic scattering states DSM 1 and DSM 2. The convection and magnetic field bias this initial state so that the subsequent decay of the disclination loops does not obey dynamic scaling. We experimentally confirm this breakdown of dynamic scaling. [S0031-9007(97)04577-8]

PACS numbers: 61.30.Gd, 47.65.+a, 61.30.Jf, 64.60.Ht

Systems quenched from a disordered to an ordered state often evolve patterns of some characteristic size as they return to equilibrium. The challenge is to describe the temporal evolution of these patterns, which can often be described by a scaling relation. The best known example of such a transition is phase separation in binary mixtures undergoing spinodal decomposition in which domains grow with a power law dependence. In this example the system has discrete symmetry and a conserved order parameter. More recently, attention has focused on systems with continuous symmetry and nonconserved order parameters in which line defects (strings or disclinations) form as a result of the quench. Such systems have been studied theoretically [1–4], numerically [5], and with computer simulations [6] which predict that the defect density scales as $t^{-\phi}$, where the exponent depends on details of the order parameter and the spatial dimensionality. Experimental realizations include liquid crystals undergoing a pressure quench [7–10] from the isotropic to nematic phase and coarsening of domains in twisted nematic films [11,12] under temperature quenches in which defect density exhibits the predicted dynamic scaling.

Recent theoretical work [13] and computer simulations [14] have considered the evolution of defects resulting from a quench in which the disordered state is biased by some field which favors a particular state in the ordered phase. The bias causes the system's evolution to no longer be described by a simple power law. The length of the defects is instead predicted to behave as $l(t) \sim (t)^{-\phi} \exp[-\gamma(t)^{\delta}]$, where the exponent ϕ depends on the nature of the order parameter and δ depends on the spatial dimensionality. The decay constant γ is a nontrivial function of the bias field such that power law behavior is recovered when the bias is removed. An experiment [15] involving the relaxation of biased twist regions in nematic liquid crystals showed agreement with the functional form of the above equation but no values for exponents were reported.

In this Letter, we report on an experimental study of the decay of disclination loops formed by a nematic liquid crystal undergoing electrohydrodynamic convection [16] with the convecting flow field acting as the bias field. These disclination loops, which are topological defects whose circumference is a disclination line that separates regions of opposite twist, do not obey dynamic scaling as they decay, in contrast to loops formed by pressure or temperature quenches from the isotropic to the nematic phase.

These disclination loops appear as roughly circularly shaped regions whose circumference, the disclination line, appears dark. Nematic disclination loops belong to the universality class of a nonconserved Ising system [7] with the closed disclination line acting similarly to a domain wall separating two regions of magnetic orientation. The recent nonbiased quench experiments and simulations show that the decay of the length of the disclination lines (the circumference of all the loops) is described by a power law with an exponent of $\frac{1}{2}$ for a three-dimensional system.

In our experiment, the nematic liquid crystal MBBA (4′-methoxybenzylidene-4-*n*-butylaniline) is sandwiched between two transparent conducting electrodes with a spacing of 135 μm. The temperature of the sample is controlled at 27 $\pm$ 0.1 °C. The cutoff frequency for this sample is approximately 300 Hz, and we work at 50 Hz to remain in the conduction regime and to avoid dc effects.

The sample is aligned by a magnetic field which provides a bulk aligning force in contrast to surface alignment techniques in which the order penetrates into the bulk. The magnetic field is applied in the plane of the sample so that the magnetic field is perpendicular to the electric field (Fig. 1). The magnetic field, through the sample's positive diamagnetic anisotropy, attempts to align the nematic director in the plane of the sample along the magnetic field direction in competition with the electric field which induces alignment along the electric field direction through the Carr-Helfrich mechanism [17]. The sample is viewed along the electric field direction using a long working distance microscope and a CCD camera.

It is important to note that the magnetic field, which at its simplest level simply aligns the director, also produces some unexpected results which we have reported elsewhere, including traveling waves [18] and the formation

 0031-9007/97/79(21)/4206(4)$10.00

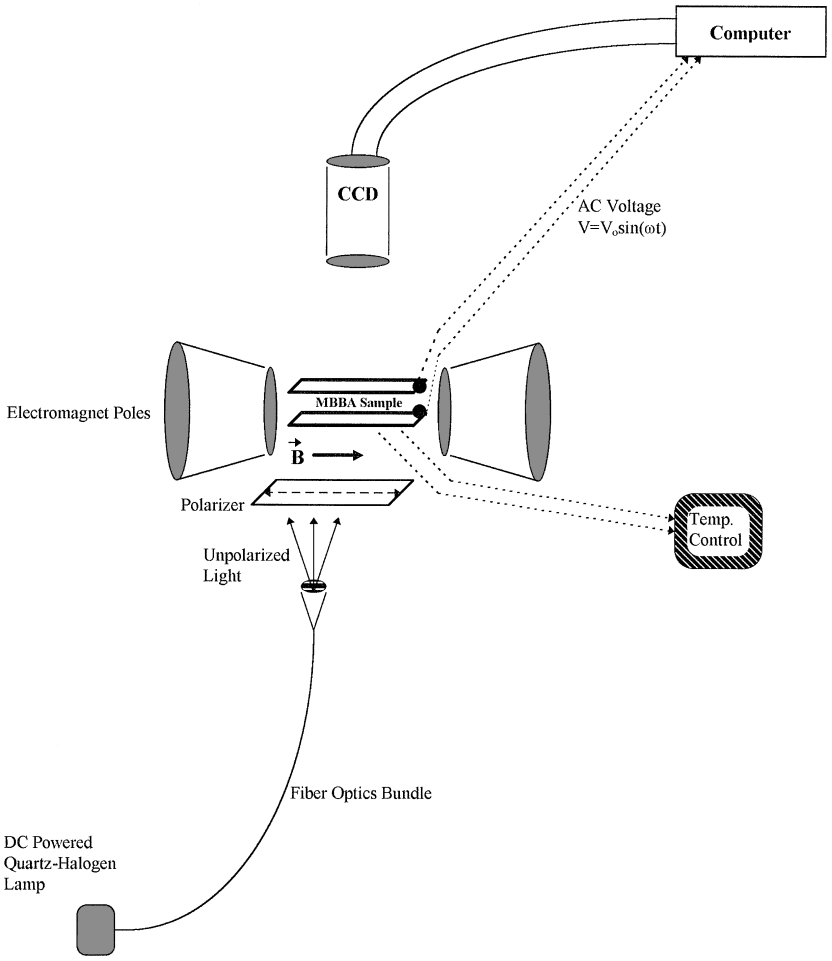

FIG. 1. Experimental arrangement.

of a surface bend-splay wall at both electrodes [19]. This latter result is important to this investigation as this surface wall, once formed, persists indefinitely. The samples discussed in this Letter all have this surface state during the experiments, even with the magnetic field removed. The effects on samples without the surface wall are ongoing.

As the applied voltage increases, the liquid crystal undergoes a series of pattern forming transitions including a transition to a turbulent state known as dynamic scattering mode 1 (DSM 1) [20] while further increase in voltage leads to a transition to another turbulent state DSM 2 [21]. It is in these DSM states that significant numbers of disclination loops are generated. With our magnetic field applied, the anisotropy between DSM 1 and 2 is removed [19] and the only difference between the two states is that DSM 2 scatters more light than the DSM 1 state because it consists of a denser jumble of disclination loops [22]. These disclination loops are somewhat difficult to observe during convection but are easily studied by turning the electric field off. Removal of the electric field reveals disclination loops while no other topological defects such as free strings are observed, indicating that we are in a strongly biased regime [14]. These disclinations then shrink away, leaving a homogeneous state with the director aligned along the magnetic field direction. Figure 2 shows the disclination loops $\frac{1}{30}$ of a second after removal of the electric field. The left hand side of the figure shows the more dense loops formed from DSM 2 while the right hand side shows loops formed from DSM 1. The magnetic field of 0.8 T remained on during the decay. In addition to the obvious density differences shown in Fig. 2, the disclination loops spawned from DSM 2 take a significantly longer time to decay than DSM 1 produced loops (Fig. 3).

This data is obtained by measuring the transmitted intensity in each $\frac{1}{30}$ of a second video frame. We correlate an increased transmitted intensity with decreased circumference of disclination loops. We make this correlation in the following way: First, the disclination loops show up as well defined shapes with a dark circumference. The circumference appears dark as the disclination line strongly backscatters light (i.e., it appears bright in reflected light). The amount of transmitted light is then decreased due to the presence of this dark loop and the decrease is proportional to the circumference of the loop. We first measure the transmitted intensity I_0 in the absence of any defects or convection. Under convection the transmitted light is greatly reduced to some value $I(t)$. The electric field is then turned off and the transmitted intensity grows, as the disclination loops shrink to I_0. We then take $I_0 - I(t)$

FIG. 2. Disclination loops spawned from DSM 2 (left) and DSM 1 (right) $\frac{1}{30}$ of a second after removal of the electric field. The two states are shown together to contrast loop density.

as proportional to the total length of all the disclination loops in view. This method underestimates the disclination length by not counting regions where the three dimensional disclination loops appear to cross in our two dimensional view. We count these crossings at the earliest times, when the effect is at its maximum, and estimate that the error is of the order of 0.1% for DSM 2 and much smaller for the less dense DSM 1 state. Because of the large number of pixels in the image (10^4), the stability of the light source and the relatively small camera noise, the random error bars are smaller than the data points.

The disclination loops appear to be confined to two dimensional layers near the surfaces, which helps explain the small number of apparent crossings we observe. This localization is expected both because loops are more easily formed at surfaces due to energy considerations [23] and because loops will be convected to the surfaces by the flow cells.

The formation and decay of disclination loops represents a biased quench in which two length scales are important; the average loop size, which decays slowly in time, and the interloop separation, which decays exponentially fast [14]. The resulting breakdown of dynamic scaling is predicted by Toyoki and Honda [13] in which the defect string length $l(t)$ decays as

$$l(t) \sim (t + \alpha)^{-\phi} \exp[-\gamma(t + \alpha)^{\delta}]. \qquad (1)$$

The exponent $\delta = d/2$, where d is the spatial dimensionality. The time exponent ϕ is expected to be $\frac{1}{2}$ for nematic disclination loops which belong to the universality class of nonconserved Ising systems. The α term results from the finite length of defects in the initial state. The degree of bias is introduced through the γ term.

The theory and simulations assume that the source of the bias is removed as soon as the system starts relaxing. Of our two sources of bias, the magnetic field and flow induced shear, only the latter is removed when the electric field is turned off. The continued presence of a bias field

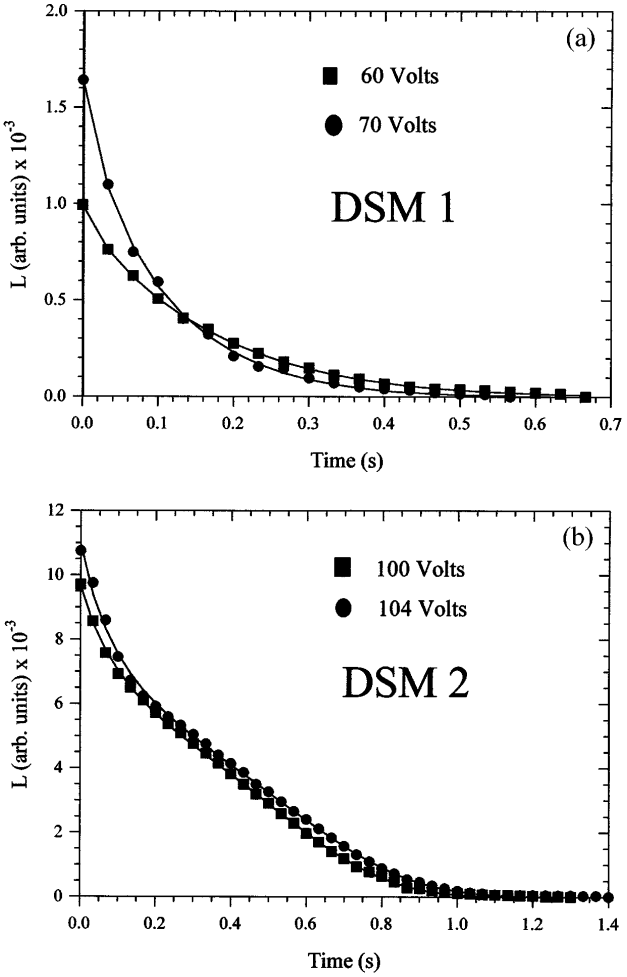

FIG. 3. Decay of the total length of disclination loops in a 0.8 T magnetic field after removal of the electric field; (a) DSM 1 at 60 and 70 V and (b) DSM 2 at 100 and 104 V. The symbols are the data points, and the solid line is the fit to Eq. (1) with ϕ fixed at 0.5 and δ at 1.5 for (a) and δ at 3.80 (104 V) and 3.95 (100 V) for (b).

is expected to have a limited role in the dynamics as its primary role is in setting up the initial conditions [5].

With a magnetic field of 0.8 T applied, decay of disclination loops from neither DSM 1 nor DSM 2 can be fit by a simple power law with any exponent. We fit Eq. (1) to our decay data (Fig. 3). For the DSM 1 state, a good fit is achieved by fixing the exponent $\phi = 0.5$ and $\delta = 1.5$. Fixing $\delta = 1$ results in a statistically worse fit, the sum of squared deviations is over twice as large as when $\delta = 1.5$.

The decay from the DSM 2 state cannot be well fit with both exponents fixed at the expected values. Holding $\phi = 0.5$, while letting δ increase to approximately 4, results in good fits as seen in Fig. 3(b). In order to determine the actual values of the exponents we allow all of the parameters to vary and give the results in Table I along with the correlated 95% confidence limits. Clearly, the uncertainty range is sufficiently large that the actual values of the exponents cannot be determined. Table I does confirm our previously stated result, namely, that while the decay from

TABLE I. Fitting results of expression (1) to decay of disclination loops. Uncertainties are 95% confidence limits. The coefficient of determination gives the fraction of the total variance accounted for by the model.

Applied voltage (V)	State	α (s)	ϕ	γ (s^{-1})	δ	Coefficient of determination
60	DSM 1	0.02 ± 0.08	0.15 ± 0.5	6.8 ± 1	1.3 ± 0.4	99.96%
70	DSM 1	0.06 ± 0.4	0.5 ± 5	7.9 ± 8	1.3 ± 4	99.91%
98	DSM 2	0.12 ± 0.07	0.6 ± 0.2	2.9 ± 0.8	4 ± 1	99.96%
100	DSM 2	0.08 ± 0.01	0.40 ± 0.06	2.9 ± 0.3	3.5 ± 0.4	99.98%
104	DSM 2	0.12 ± 0.08	0.6 ± 0.2	1.8 ± 0.7	4 ± 1	99.90%

the DSM 1 state is well described by the Toyoki and Honda expression with the expected exponents the DSM 2 state is fit by the same equation but requires significantly larger values of δ. (Fixing the exponents at the values shown in Fig. 3 decreases the coefficient of determination by 0.01% from the best fit values.)

The decay of the DSM 2 spawned loops are not well fit by Eq. (1) with the expected exponents. What makes the loops from DSM 2 different from their DSM 1 counterparts? Either these loops are inherently different or the interactions between loops, resulting from their increased density, lead to deviations from the theory which ignores interaction events. If the decay is affected by the density of loops, the behavior of DSM 2 originated loops should be identical to that of the DSM 1 type loops when the density of DSM 2 loops falls to a sufficiently low level. Figure 3 shows that the disclination loops from DSM 2 are approximately 5 times more turbid than the DSM 1 state. When the turbidity of the DSM 2 spawned disclination loops falls to a similar density the resulting decay is also well fit by Eq. (1) with the expected exponents. This result indicates that the deviation between theory and experiment is likely due to interactions between disclination loops which are not accounted for in the original theory. That the variation occurs in the δ exponent is consistent with this view as this exponent controls how the interloop separation grows.

In summary, we measured the decay of line defects formed from electrohydrodynamic convection of a nematic liquid crystal. We find that the decay does not follow dynamic scaling but instead is well fit by the Toyoki and Honda theory when the defect density is sufficiently low. We also verify that the interactions of defects is important at high defect density, as exhibited in the DSM 2 state, and must be accounted for to accurately describe the decay.

J. P. M. thanks Nigel Goldenfeld for useful correspondence and Martin Zapotocky for helpful conversations.

[1] G. F. Mazenko and M. Zannetti, Phys. Rev. B **32**, 4565 (1985).
[2] F. de Pasquale and P. Tartaglia, Phys. Rev. B **33**, 2081 (1986).
[3] H. Toyoki and K. Honda, Prog. Theor. Phys. **78**, 237 (1987).
[4] A. J. Bray, Phys. Rev. Lett. **62**, 2841 (1989).
[5] H. Nishimori and T. Nukii, J. Phys. Soc. Jpn. **58**, 563 (1988).
[6] M. Mondello and N. Goldenfeld, Phys. Rev. A **42**, 5865 (1990).
[7] I. Chuang, B. Yurke, and A. N. Pargellis, Phys. Rev. E **47**, 3343 (1993).
[8] B. Yurke, A. N. Pargellis, and I. Chuang, Physica (Amsterdam) **178B**, 56 (1992).
[9] I. Chuang, N. Turok, and B. Yurke, Phys. Rev. Lett. **66**, 2472 (1991).
[10] I. Chuang, R. Durrer, N. Turok, and B. Yurke, Science **251**, 1336 (1991).
[11] H. Orihara and Y. Ishibiashi, J. Phys. Soc. Jpn. **55**, 2151 (1986).
[12] T. Nagaya, H. Orihara, and Y. Ishibiashi, J. Phys. Soc. Jpn. **56**, 3086 (1987).
[13] H. Toyoki and K. Honda, Phys. Rev. B **33**, 385 (1986).
[14] M. Mondello and Nigel Goldenfeld, Phys. Rev. A **45**, 657 (1992).
[15] T. Nagaya, H. Orihara, and Y. Ishibiashi, J. Phys. Soc. Jpn. **59**, 377 (1990); in *Geometry and Thermodynamics—Common Problems of Quasi-Crystals, Liquid Crystals, and Incommensurate Systems*, edited by J. C. Toledano, NATO ASI Ser. B Vol. 229 (Plenum, New York, 1990).
[16] See, for instance, P. G. de Gennes and J. Prost, *The Physics of Liquid Crystals* (Oxford, New York, 1993), 2nd ed; S. Chandrasekhar, *Liquid Crystals* (Cambridge, New York, 1992), 2nd ed.
[17] E. F. Carr in *Ordered Fluids and Liquid Crystals*, Advances in Chemistry Series 76 (American Chemical Society, Washington, DC, 1967); W. J. Helfrich, J. Chem. Phys. **51**, 4092 (1969). Also see Ref. [16] for a general introduction.
[18] J. P. McClymer, Mol. Cryst. Liq. Cryst. **199**, 233 (1991); E. F. Carr and J. P. McClymer, Mol. Cryst. Liq. Cryst. **182B**, 245 (1990); E. F. Carr, Mol. Cryst. Liq. Cryst. Lett. **8**, 117 (1992).
[19] J. P. McClymer, E. F. Carr, and H. Shehadeh, in *Spatio-Temporal Patterns*, edited by P. E. Cladis and P. Palffy-Muhoray, Proceedings of the SFI Studies in the Science of Complexity (Addison-Wesley, Reading, MA, 1994), Vol. XXI, p. 367.
[20] G. H. Helimeier, L. A. Zanoni, and L. Barton, Proc. IEEE **56**, 1162 (1968); A. P. Kapustin and L. K. Vistin, Kristallografiya **10**, 118 (1965); G. Elliot and J. G. Gibson, Nature (London) **205**, 995 (1965).
[21] A. Sussmann, Appl. Phys. Lett. **21**, 269 (1972).
[22] W. Zimmerman, MRS Bull. **16**, 46 (1991).
[23] P. G. de Gennes, in *Molecular Fluids*, edited by Balian Weill (Gordon and Breach, New York, 1976); J. Phys. (Paris), Lett. **35L**, 271 (1974).